HHS Public Access

Author manuscript

J Bone Miner Res. Author manuscript; available in PMC 2016 November 01.

Published in final edited form as:

J Bone Miner Res. 2015 November ; 30(11): 1959–1968. doi:10.1002/jbmr.2556.

PTH-IGF SIGNALING PROMOTES BONE FORMATION THROUGH GLYCOLYSIS:

PTH Promotes Bone Anabolism by Stimulating Aerobic Glycolysis via IGF Signaling

Emel Esen[1,2], **Seung-Yon Lee**[2], **Burton M Wice**[3], and **Fanxin Long**[1,4]

[1]Division of Biology and Biomedical Sciences, Washington University School of Medicine, St. Louis, MO, USA

[2]Department of Orthopaedic Surgery, Washington University School of Medicine, St. Louis, MO, USA

[3]Department of Medicine, Washington University School of Medicine, St. Louis, MO, USA

[4]Department of Developmental Biology, Washington University School of Medicine, St. Louis, MO, USA

Abstract

Teriparatide, a recombinant peptide corresponding to amino acids 1-34 of human parathyroid hormone (PTH), has been an effective bone anabolic drug for over a decade. However, the mechanism whereby PTH stimulates bone formation remains poorly understood. Here we report that in cultures of osteoblast-lineage cells, PTH stimulates glucose consumption and lactate production in the presence of oxygen, a hallmark of aerobic glycolysis, also known as Warburg effect. Experiments with radioactively labeled glucose demonstrate that PTH suppresses glucose entry into the tricarboxylic acid cycle (TCA cycle). Mechanistically, the increase in aerobic glycolysis is secondary to insulin-like growth factor (Igf) signaling induced by PTH, whereas the metabolic effect of Igf is dependent on activation of mammalian target of rapamycin complex 2 (mTORC2). Importantly, pharmacological perturbation of glycolysis suppresses the bone anabolic effect of intermittent PTH in the mouse. Thus, stimulation of aerobic glycolysis via Igf signaling contributes to bone anabolism in response to PTH.

Keywords

PARATHYROID HORMONE; PTH; BONE ANABOLISM; AEROBIC GLYCOLYSIS; IGF

Address correspondence to: Fanxin Long, Department of Developmental Biology, Washington University School of Medicine, St. Louis, MO 63110, USA. flong@wustl.edu.

Additional Supporting Information may be found in the online version of this article. Journal of Bone and Mineral Research, Vol. XX, No. X, Month 2015, pp XXXX–XXXX DOI: 10.1002/jbmr.2556

Disclosures

All authors state that there are no conflicts of interest.

Introduction

Daily injections of either full-length (amino acid 1-84) or a fragment of parathyroid hormone (PTH; amino acid 1-34, known as teriparatide), known as the intermediate treatment regimen, increase bone formation and reduce incidences of fractures in osteoporotic patients.[1] Extensive studies have indicated that PTH stimulates bone anabolism through direct regulation of osteoblast-lineage cells at multiple levels; these include enhancement of osteoblast activity, stimulation of osteoblast differentiation, attenuation of osteoblast apoptosis, and activation of quiescent bone-lining cells.[2–5] However, the molecular mechanism mediating the various regulations by PTH is not fully understood.

PTH is known to signal through the PTH 1 receptor (PTH1R), a G-protein–coupled receptor.[6] PTH1R signaling initiates $G\alpha_s$-mediated activation of adenylyl cyclase resulting in cAMP production, as well as $G\alpha_{q/11}$-mediated activation of phospholipase C (PLC) and subsequently protein kinase C (PKC). In addition, PTH activates extracellular regulated kinase (ERK) signaling through either G proteins or β-arrestin.[7] PTH (1–31), which mainly activates cAMP production, produces an equivalent anabolic effect to PTH (1-34), whereas PTH (3–34), stimulating PKC but not cAMP production, does not exhibit a similar effect, indicating that $G\alpha_s$/cAMP signaling is primarily responsible for the bone anabolic function of PTH.[8] More recently, PTH signaling has been shown to engage the Wnt co-receptor Lrp6 and the TGFβ type II receptor. In particular, PTH binding to PTH1R induces formation of a ternary complex with Lrp6, resulting in cAMP production and PKA-dependent β-catenin stabilization.[9,10] On the other hand, TGFβ type II receptor appears to mitigate PTH-cAMP signaling though endocytosis of PTH1R.[11] A major output of PTH-cAMP signaling is increased synthesis and release of insulin-like growth factor 1 (Igf1) by osteoblast-lineage cells.[12–14] Importantly, deletion of either Igf1 or Igf1r in osteoblasts essentially abolishes the bone anabolic effect of PTH in mice, thus highlighting the importance of Igf signaling in PTH function.[15–17] However, how PTH-Igf signaling exerts the bone anabolic effect remains unclear.

Recent studies have implicated cellular glucose metabolism in the regulation of osteoblast biology.[18] In particular, Wnt-Lrp5 signaling, a potent bone anabolic mechanism, stimulates aerobic glycolysis in osteoblast lineage cells, whereas upregulation of glycolysis promotes bone formation in the mouse.[19,20] Interestingly, PTH has been known to stimulate glycolysis in bone long before it was used a bone anabolic agent.[21–23] However, a direct link between glycolysis and bone anabolism in response to PTH has not been made.

Here we report that PTH stimulates aerobic glycolysis while suppressing glucose oxidation through the tricarboxylic acid cycle (TCA cycle) in osteoblast lineage cells. The metabolic reprogramming by PTH is mediated by Igf–phosphatidylinositol-3′-kinase (PI3K)–mammalian target of rapamycin complex 2 (mTORC2) signaling. Importantly, suppression of the metabolic changes initiated by PTH diminishes its bone anabolic function in the mouse. Thus, stimulation of aerobic glycolysis appears to be an important mechanism underlying the anabolic effect of PTH.

Materials and Methods

Mice

The Ldha mouse strain (Ldha$^{tm1a(EUCOMM)Wtsi}$) was purchased from the International Knockout Mouse Consortium (KOMP). To obtain the Ldha^{f} allele, the mouse was crossed with the R26-FLP mouse (B6.129S4-Gt(ROSA)26Sor$^{tm1(FLP1)Dym}$/RainJ) (Jackson Laboratories, Bar Harbor, ME, USA). The wild-type and floxed Ldha alleles were genotyped by PCR using the following primers: 5′-TCGTGGTATCGTTATGCGCC-3′, 5′-CTCGCTTGCCTTATGGGTTC-3′, and 5′-TGGCAGTCAAGTCTCCAAGAAG-3′; this produced a fragment of 199 bp from the floxed allele and that of 382 bp from the wild-type allele. Igf1r$^{f/f}$ mice (B6;129-*Igf1r*^{tm2Arge}/J) were purchased from Jackson Laboratories.[24] Washington University Animal Studies Committee approved all mouse experiments.

Analyses of postnatal skeleton

Micro–computed tomography (μCT) analyses were performed with Scanco μCT 40 (Scanco Medical AG, Brüttisellen, Switzerland) as described.[25,26] Quantification of the trabecular bone in the tibia was performed with 35 μCT slices (total of 0.56 mm) right below the growth plate with the threshold set at 250. For cortical bone, 50 slices from the midshaft were analyzed with the same threshold.

Histology and histomorphometry was performed as described, with the exception that the mice were not perfused prior to euthanasia.[25] For dynamic histomorphometry, mice were injected intraperitoneally with calcein (20 mg/kg; Sigma, St. Louis, MO, USA) at 10 and 2 days before euthanasia. For serum-based biochemical assays, mice were first fasted for 6 hours and then anesthetized with xylazine/ketamine mix before blood collection in serum separator tubes (cat# 365956; BD Biosciences, San Jose, CA, USA). Blood was incubated at room temperature for 30 min, spun down for 5 min before serum was collected. Serum CTX-I assay was performed using the RatLaps ELISA kit (Immunodiagnostic Systems, Ltd., Boldon, UK). Serum lactate was measured with a lactate assay kit (cat# 1200011002; Eton Biosciences, San Diego, CA, USA).

Calvarial osteoblast culture

Frontal and parietal bones dissected from newborn mice (0 to 5 days old) were rinsed three times with PBS before being subjected to four rounds of digestion with 1.8 mg/mL collagenase (catalog # C0130; Sigma-Aldrich) at 37°C, with the first round for 10 min, and the subsequent rounds for 15 min each. The supernatant from the first digestion was discarded, but cells from the subsequent digestions were collected, strained through 70-μM filters and plated in α-MEM with 20% FBS and 1% Pen Strep.

Antibodies

Antibodies for P-Akt (S473) (cat#9271), Akt (cat#9272), β-actin (cat#4970), p-NDRG1-Thr346 (cat#3217S), LDHA (2012), and p-IGF1R (3027) were purchased from Cell Signaling Technologies (Danvers, MA, USA). Hk2 (sc-6521), Ldha (sc-27230) and α-tubulin (sc-8035) primary antibodies, and horseradish peroxidase (HRP)-conjugated anti-mouse (sc-2005) or anti-goat (sc-2352) secondary antibodies were from Santa Cruz

Biotechnology (Dallas, TX, USA). Pdk1 (KAP-pk112) antibody was from Enzo (Farmingdale, NY, USA). HRP-conjugated anti-rabbit secondary antibody (NA934V) was from GE Healthcare (Little Chalfont, UK).

Protein extraction and Western blot

For protein extractions, femurs and tibias were isolated and cleaned of excess tissue, followed by surgical removal of the epiphyses, and removal of the marrow by centrifugation. The bones were then washed with cold PBS three times before being snap-frozen in liquid nitrogen, and subsequent pulverization in a Mikro Dismembrator U (Sartorius, Gottingen, Germany). Protein was extracted with 150 μL radioimmunoprecipitation assay (RIPA) buffer (cat# R0278; Sigma-Aldrich) containing phosphatase inhibitors (cat# 04906845001; Roche, Nutley, NJ, USA) and proteinase inhibitor (cat# 11836170001; Roche) on ice for 30 min. Protein concentration was measured with BCA assay (Thermo Scientific, Waltham, MA, USA), and Western blotting was performed according to standard protocols.

qRT-PCR

RNA was extracted with RNeasy kit, followed by RNase-free DNase kit according to manufacturer's instructions (Qiagen, Limburg, Netherlands). RNA concentration was measured with NanoDrop 2000 (Thermo Scientific). One microgram (1 μg) of RNA was used to make cDNA with iScript cDNA synthesis kit (Bio-Rad Laboratories, Hercules, CA, USA). Two microliters (2 μL) of cDNA diluted at 1:10 was used for each reaction with Fast-start SYBR green (Bio-Rad) and 0.05 μM each of forward and reverse primers. Technical duplicates were prepared for each biological sample. StepOnePlus Real Time PCR Systems (Applied Biosystems, Inc., Foster City, CA, USA) was used with a protocol starting with 3 min at 95°C, followed by 40 cycles and ending with a melt curve. 18S ribosomal RNA was used for normalization. The primer sequences are shown in Supporting Table 1.

Cell culture and metabolic measurements

MC3T3-E1 (subclone 4) cells were maintained in ascorbic acid-free α-MEM medium (a10490-01; Gibco, Grand Island, NY, USA) and switched to complete α-MEM (cat#12561; Gibco) for experiments. Both media were supplemented with 10% heat inactivated FBS (Gibco) and Pen Strep (cat#14140; Gibco). The mineralization media contained additional supplements: 100 nM dexamethasone, 50 μg/mL ascorbic acid, and 10 mM β-glycerol phosphate. PTH (1-34), PTH (3-34), and PTH (1-31) were obtained from Bachem Biosciences (Torrance, CA, USA). All PTH fragments were dissolved in a sterile aqueous solution containing 0.9% NaCl, 0.1% BSA, 0.001 N HCl, and used as 500 ng/mL unless otherwise indicated. This solution was used as vehicle control in all PTH experiments. Recombinant mouse Dkk1, recombinant mouse Frizzled-8 Fc chimera and Igf1 were used at 500 ng/mL (R&D systems, Minneapolis, MN, USA). For Dkk1 experiments only, cells were pretreated with Dkk1 for 30 min before the addition of PTH. The chemical inhibitors used are as follows: LY294002 (Sigma Aldrich), rapamycin (Sigma Aldrich), MK-2206 (Selleckchem, Houston, TX, USA), GSK650394 (Tocris Biosciences, Bristol, UK), EMD638683 (MedChem Express, Monmouth Junction, NJ, USA), OSI-906 (ie, linsitinib) (Selleckchem), picropodophyllotoxin (Tocris), U-73122 (Calbiochem, San Diego, CA, USA), Ro 31-8220 (Sigma Aldrich), PD98059 (Sigma Aldrich), and U0126 (Cell signaling).

Glucose and lactate measurements were done as described.[20] For glucose uptake assays, cells were plated in 96-well clear-bottom culture plates the day before the experiment. The cells were stimulated with PTH for the indicated time before switching to fresh medium containing 100 μM fluorescent deoxyglucose derivative (2-NBDG) for 30 min, followed by preparation for fluorescence reading according to the manufacturer's instructions (Glucose Uptake Cell-based Assay Kit; Cayman Chemical). 2-NBDG uptake was measured at 485/535 nm (excitation/emission) using a plate reader (BioTek model SAMLFTA, Gen5 software). Fluorescence intensity was normalized to the protein content in each well.

For Seahorse extracellular flux assays, undifferentiated or differentiated MC3T3-E1 cells were plated at 5000 or 10,000 cells/well, respectively, in XF96 plates coated with Cell-Tak (BD Biosciences). On the next day, the cells were treated with 500 ng/mL PTH or Igf1 for indicated time with or without inhibitors, then switched to Assay Medium (Seahorse cat# 101022-100 or Sigma D5030-1L) and further incubated in CO_2-free incubator for 1 hour. Oligomycin (ATP synthase inhibitor), carbonyl cyanide p-trifluoromethoxyphenylhydrazone (FCCP; proton ionophore), antimycin A (complex III inhibitor), and rotenone (complex I inhibitor) (Seahorse Stress Kit) were prepared in XF assay medium with final concentration of 5 μM for oligomycin and 1 μM for the rest. At the end of the assays, protein concentrations were measured for normalization of oxygen consumption rate (OCR) and extracellular acidification rate (ECAR).

shRNA knockdown and adenovirus infection

Lentiviral shRNA expression constructs were purchased from the Genome Center at Washington University. Targeting sequences are as follows: Gfp: 5′-TGACCCTGAAGTTCATCTGCA-3′, Ldha: 5′-CGTGAACATCTTCAAGTTCAT-3′. Lentivirus was prepared as described.[20] Adenovirus expressing Gfp (ad-Gfp) or Cre (ad-Cre) was purchased from the Gene Transfer Vector Core at the University of Iowa. Subconfluent calvarial cells were infected overnight with ad-Gfp or ad-Cre at 50 multiplicity of infection (MOI) in media containing 2% serum, and then cultured in media containing 10% serum for 72 hours before PTH treatment.

In vivo PTH treatment

Three-month-old C57BL/6J male mice were injected intraperitoneally with either 80 μg/kg PTH (1-34) or the vehicle control 5 days per week for 1 month. Sodium dichloroacetate (DCA) (Sigma) was delivered through drinking water at the concentration of 2 g/L and with pH adjusted to approximately 7.2. For studies of signaling events in vivo, PTH (1-34) or vehicle was injected intraperitoneally at the indicated concentration and the bones were harvested 6 or 12 hours after injection. Bone protein extracts were prepared from femurs and tibias as described earlier.

CO_2 trap experiments

MC3T3-E1 cells were plated in flasks at a concentration of 4×10^5/flask (cat# 353107; Becton Dickinson, Franklin Lakes, NJ, USA) and treated with mineralization medium for 3 days before being subjected to the CO_2 trap procedure as described.[27] Briefly, the flasks were refitted with collection tubes (#211-0059; VWR, Radnor, PA, USA) bearing holes on

the sides, and sealed with rubber stoppers (cat # FB57873 and cat # FB57877; Fisher Scientific, Waltham, MA, USA). The cells were incubated in regular media containing 2 μ1 of 0.1 mCi/mL ^{14}C-labeled glucose (total radioactivity 444,000 disintegrations per minute [dpm]), with or without PTH, in the sealed CO_2 trap system for 24 hours. [$^{14}C_1$]-Glc (cat# ARC 0120C), [$^{14}C_{3,4}$]-Glc (cat# ARC 0211A), and [$^{14}C_6$]-Glc (cat# ARC 0121B) were from American Radiolabeled Chemicals (St. Louis, MO, USA). Afterward, 2.5 mL of 2.5 M H_2SO_4 was injected into the flask, and 1 mL of 2% NaOH into the collection tube. After overnight incubation at room temperature, solution in the tube was collected and measured for radioactivity with a scintillation counter. A parallel experiment was conducted with identical treatments for cell counting. For glucose consumption, an aliquot of the medium was measured before the injection of H_2SO_4.

Statistical analyses

All two-group comparisons were performed with Student's *t* test. For the multigroup comparisons in the PTH experiment in vivo, two-way factorial ANOVA for independent samples was performed (http://vassarstats.net). Statistical significance was determined by a p value <0.05.

Results

PTH stimulates aerobic glycolysis in osteoblast-lineage cells

To evaluate the effect of PTH on glucose metabolism in osteoblast-lineage cells, we used the preosteoblastic cell line MC3T3-E1 as a model system. We first determined glucose consumption by measuring glucose levels remaining in the culture media after various times of incubation with PTH (1-34) (hereafter referred to as PTH) at different concentrations. Whereas PTH at 50 ng/mL did not have an effect, it significantly increased glucose consumption at 100 or 250 ng/mL after 48 hours (Supporting Fig. 1A). 500 ng/mL PTH had a greater effect, but 1 μg/mL PTH did not further increase glucose consumption (Supporting Fig. 1B). With 250 ng/mL PTH, the increase in glucose consumption over the control was progressive with time and became statistically significantly after 48 hours (Fig. 1*A*, Supporting Fig. 1C). The increased glucose consumption was unlikely due to changes in cell proliferation or viability, because PTH did not significantly alter the number or protein content of the cells (Supporting Fig. 1D). Incubation with 2-NBDG confirmed that PTH increased glucose uptake progressively after 24 and 48 hours (Fig. 1*B*). Because PTH was previously shown to signal more robustly in MC3T3-E1 cells upon differentiation, we examined the effect on glucose after 3 days of differentiation in the presence of ascorbic acid and beta-glycerophosphate.[28] Compared to the undifferentiated counterpart, the differentiated MC3T3-E1 cells consumed more glucose under the basal condition, but more importantly, significantly increased glucose consumption after 6 or 24 hours of PTH treatment (Fig. 1*C*). The stimulatory effect of PTH on glucose consumption was confirmed with primary calvarial cells isolated from newborn mice (Fig. 1*D*). Thus, PTH stimulates glucose utilization by osteoblast-lineage cells in vitro.

To directly assess the effect of PTH on cellular metabolism, we examined MC3T3-E1 cells with the Seahorse extracellular flux analyzer. PTH treatment for 24 hours notably enhanced

OCR both under basal conditions and in response to the mitochondria stressors (Fig. 1*E*). In particular, PTH increased basal respiration, ATP production, and spare respiratory capacity of the mitochondria (Supporting Fig. 2A). PTH also stimulated the ECAR, which was likely due to greater lactate production, as indicated by the higher lactate concentration in the media (Fig. 1*F, G*; Supporting Fig. 2B). Compared to MC3T3-E1 cells, the primary calvarial cells exhibited a more pronounced increase in media lactate levels in response to PTH (Fig. 1*G*). Similarly, when added to differentiated MC3T3-E1 cells, PTH markedly increased lactate levels in the media after 6 or 24 hours. Thus, PTH stimulates both mitochondrial respiration and lactate production in osteoblast-lineage cells.

The observed changes in cellular metabolism prompted us to examine the effect of PTH on the metabolic fates of glucose in differentiated MC3T3-E1 cells. We used a CO_2 trapping method to capture radioactive $^{14}CO_2$ produced from glucose labeled with ^{14}C at specific positions (Supporting Fig. 3A). In this method, [$^{14}C_{3,4}$]-glucose produces $^{14}CO_2$ upon entering the TCA cycle via the conversion of pyruvate to acetyl-coenzyme A (CoA), whereas [$^{14}C_1$]- or [$^{14}C_6$]- glucose generates $^{14}CO_2$ through the second round of the TCA cycle. Because [$^{14}C_1$]-glucose also produces $^{14}CO_2$ through pentose phosphate pathway (PPP), the PPP flux is calculated by subtracting [$^{14}C_6$]-glucose-derived $^{14}CO_2$ from [$^{14}C_1$]-glucose-derived $^{14}CO_2$ (Supporting Fig. 3B). We confirmed that in the CO_2 trapping system, PTH stimulated glucose consumption and lactate production after 24 hours (Supporting Fig. 3C). Remarkably, despite the increase in total glucose consumption, the amount of glucose entering the TCA cycle as reflected by the total $^{14}CO_2$ radioactivity released from [$^{14}C_{3,4}$]-glucose was reduced by ~44% in response to PTH. By normalizing the $^{14}CO_2$ radioactivity to total radioactivity uptake (herein termed $^{14}CO_2$ production rate), we found that under basal conditions, ~19% of glucose entered the TCA cycle via pyruvate decarboxylation with ~7% (2 × $^{14}CO_2$ production rate from $^{14}C_6$-Glc) completing the full cycle, and that PTH reduced those numbers to ~7% and ~3%, respectively (Table 1). After normalizing the $^{14}CO_2$ production rate to the cell number (herein termed $^{14}CO_2$ production index), we determined that PTH suppressed both glucose entry to the TCA cycle and its completion through the cycle by ~60% (Supporting Fig. 3D, E). We further calculated that the $^{14}CO_2$ production rate for PPP (difference between [$^{14}C_1$]- and [$^{14}C_6$]-glucose) rose from ~1% under the basal condition to ~3% in response to PTH, representing an increase of 216% in the $^{14}CO_2$ production index (Table 1). Thus, PTH enhances both glycolysis and PPP (remaining a small percentage of total glucose consumption), but suppresses glucose entry into TCA cycle.

We next examined the molecular basis for the metabolic changes in response to PTH. PTH markedly increased the protein levels of hexokinase II (Hk2), lactate dehydrogenase A (Ldha), and pyruvate dehydrogenase kinase 1 (Pdk1) in either MC3T3-E1 cells or primary calvarial cells (Fig. 2*A*). We chose Ldha as an example to test the functional relevance of the upregulated enzymes. Knockdown of Ldha in MC3T3-E1 cells essentially abolished the induction of glucose consumption by PTH (Fig. 2*B*). Similarly, genetic deletion of Ldha in primary calvarial cells prepared from $Ldha^{f/f}$ mice with adenovirus expressing Cre blunted the PTH effect (Fig. 2*C*). Overall, the changes in the protein levels of several metabolic enzymes can account for the increase in glycolysis but decrease in glucose entry into the TCA cycle in response to PTH.

PTH stimulates aerobic glycolysis through Igf-mTORC2 signaling

We next sought to understand the signaling mechanism through which PTH stimulates glycolysis. Because PTH is known to activate $G\alpha_s$/cAMP/PKA, $G\alpha_{q/11}$/PLCβ/PKC, and ERK signaling, we first sought to distinguish the relative contribution of each pathway to the metabolic regulation. PTH (1-31), mostly activating the $G\alpha_s$ pathway, enhanced glucose consumption with similar potency to PTH (1-34) (Fig. 3*A*). In contrast, PTH (3-34), activating mostly $G\alpha_{q/11}$ signaling, did not increase glucose consumption when applied at the same concentration as PTH (1-31) or PTH (1-34), and exhibited only a minor effect at a higher concentration (Fig. 3*A*). Moreover, forskolin, known to activate adenylyl cyclase to increase intracellular cAMP levels, potently stimulated glucose consumption (Fig. 3*B*). Chemical inhibition of PLC, PKC, or ERK did not impair PTH-induced glucose consumption (Supporting Fig. 4). Thus, PTH reprograms glucose metabolism mainly through a cAMP-dependent mechanism.

PTH-cAMP signaling may stimulate glycolysis either directly or through the induction of a secondary signal. Our studies have revealed a time lag between PTH exposure and the increase in the rate of glucose uptake (Fig. 1*B*). Moreover, MC3T3-E1 cells pulsed with either PTH or forskolin for 1 hour and then cultured for 47 hours showed a similar increase in glucose consumption to those incubated with PTH or forskolin for the entire 48 hours (Fig. 3*C*). These results prompted us to hypothesize that PTH initiates a secondary signal which later functions independently to control glucose metabolism. To identify such a signal, we first examined Wnt proteins because they have been shown to stimulate aerobic glycolysis.[20] However, neither Dkk1 nor Frizzled-8 Fc, both extracellular antagonists of Wnt proteins, had any effect on glucose utilization in response to PTH (Supporting Fig. 5). In addition, PTH and Wnt3a additively increased glucose consumption in MC3T3-E1 cells (Fig. 4*A*). Thus, PTH stimulates glycolysis likely independent of Wnt signaling.

Because PTH-cAMP signaling has been shown to increase Igf1 production in osteoblast-lineage cells, we next tested the involvement of Igf in PTH-driven glycolysis.[14] Consistent with previous reports, we found that PTH increased the mRNA level of Igf1 and to a lesser extent, Igf2 in MC3T3-E1 cells within 6 hours of treatment (Fig. 4*B*).[29] Moreover, PTH induced phosphorylation of Igf1 receptor (Igf1r) at Tyr1135/1136 after 24 hours, indicating activation of Igf signaling.[30] (Supporting Fig. 6A). Importantly, chemical inhibition of Igf1r signaling blocked PTH-induced glucose consumption, phosphorylation of Igf1r, as well as Ldha and Hk2 induction in MC3T3-E1 cells (Fig. 4*C*, *D*; Supporting Fig. 6B). Similarly, in differentiated MC3T3-E1 cells, inhibition of Igf1r essentially nullified the effect of PTH on glucose consumption, ECAR, and OCAR (Fig. 4*E*, *F*). To test further the function of Igf signaling, we genetically deleted Igf1r in primary calvarial cells isolated from $Igf1r^{f/f}$ mice with an adenovirus expressing Cre. Removal of Igf1r abolished the PTH-induced glucose consumption (Fig. 4*G*). Finally, we examined directly the effect of Igf signaling on metabolism. Like PTH, Igf1 stimulated glucose consumption and lactate production by MC3T3-E1 after 48 hours of treatment (Supporting Fig. 6C). In differentiated MC3T3-E1 cells, Igf1 increased only ECAR after 6 hours of treatment, but both ECAR and OCAR after 24 hours, indicating that Igf signaling acutely activates aerobic glycolysis, and

subsequently oxidative phosphorylation (Supporting Fig. 6D, E). In summary, Igf signaling is responsible for the PTH-induced metabolic reprogramming.

We then investigated the signal transduction cascade downstream of Igf1r and responsible for the regulation of glycolysis. Igf is known to activate both mTORC1 and mTORC2 signaling downstream of PI3K. Rapamycin, which mainly inhibits mTORC1, reduced the basal level of glucose consumption by MC3T3-E1 cells, but did not impair the induction by PTH (Supporting Fig. 7A). We next examined the involvement of mTORC2, which is commonly assayed by phosphorylation of AKT at S473 and serum/glucocorticoid regulated kinase 1 (Sgk1), which in turn phosphorylates Ndrg1.[31] We found that PTH induced Ndrg1 phosphorylation markedly, and Akt-S473 phosphorylation to a lesser degree; both inductions were abolished upon Igf1r inhibition (Fig. 5*A*). Moreover, PTH (1-34) and PTH (1-31), both stimulating glycolysis, but not PTH (3-34), which does not have the property, induced phosphorylation of Ndrg1 (Fig. 5*B*). Inhibition of PI3K reduced basal level glucose consumption, and more importantly, dose-dependently suppressed the induction by PTH (Fig. 5*C*). We next evaluated the contribution of Sgk1 and Akt, both downstream effectors of mTORC2, to the PTH response. Inhibition of Sgk1 abolished the effect of PTH not only on phosphorylation of Ndrg1 and Ldha protein level, but also on glucose consumption and lactate production (Fig. 5*D*–*F*, Supporting Fig. 7B). Moreover, Sgk1 inhibition abolished Igf1-induced glucose consumption and ECAR (Fig. 5*G*, *H*). Similarly, an Akt inhibitor that suppressed the self-phosphorylation of Akt also blunted the increase in glucose consumption in response to PTH (Fig. 5*I*, *J*). Thus, PTH appears to stimulate glycolysis through both Akt and Sgk1 downstream of Igf-PI3K-mTORC2 signaling.

Increased glycolysis contributes to bone anabolic effect of PTH in vivo

We finally examined the potential contribution of metabolic reprogramming to PTH-induced bone formation in vivo. We first evaluated whether teriparatide induced similar metabolic changes as observed in vitro. Indeed, intraperitoneal injection of teriparatide dose-dependently increased the glycolytic enzymes as well as phosphorylation of Ndrg1 and Akt at S473 in bone protein extracts form 6 through 12 hours (Fig. 6*A*, Supporting Fig. 8). To assess the importance of aerobic glycolysis, we used dichloroacetate (DCA), which inhibits the activity of Pdk1, to enhance glucose metabolism in the TCA cycle. As expected, DCA suppressed teriparatide-induced glucose consumption in both undifferentiated and differentiated MC3T3-E1 cells (Supporting Fig. 9A, B). We injected teriparatide daily in 3-month-old BL6 male mice for 1 month with or without DCA co-treatment in drinking water. Teriparatide did not alter body weight whereas DCA caused a slight decrease in body weight (Supporting Fig. 9C). Consistent with increased aerobic glycolysis, teriparatide increased serum lactate levels in the mouse, but the effect was abolished by co-administration of DCA, which alone did not have an effect (Fig. 6*B*). Importantly, DCA greatly attenuated the teriparatide-induced increase in trabecular bone parameters as determined by μCT (Fig. 6*C*) (Table 2). The anabolic effect of teriparatide on cortical bone was not significant, with or without DCA (Table 3). Histology confirmed that DCA essentially reversed the increase in trabecular bone mass caused by teriparatide (Fig. 6*D*). Thus, suppression of aerobic glycolysis through activation of glucose metabolism in the TCA cycle diminishes the anabolic role of PTH.

We next investigated the cellular basis underlying the DCA effect. Histomorphometry revealed that DCA dampened the increase in osteoblast number, mineral apposition rate (MAR), and bone formation rate (BFR/BS) caused by PTH (Fig. 6*E*, *F*; Supporting Fig. 8D). On the other hand, DCA did not alter the PTH-induced increase in serum CTX-I levels, an indicator of total osteoclast activity (Fig. 6*G*). Overall, increased aerobic glycolysis is necessary for PTH to stimulate osteoblast number and function in vivo.

Discussion

We have uncovered an important role for aerobic glycolysis in mediating the bone anabolic function of PTH. We show that PTH stimulates aerobic glycolysis but suppresses mitochondrial metabolism of glucose. The metabolic regulation by PTH is mediated through induction of Igf signaling that acts via PI3K and mTORC2 (Fig. 6*H*). Importantly, pharmacological suppression of aerobic glycolysis blunts the bone anabolic function of PTH in vivo. The work not only confirms and extends the historic studies about the effect of PTH on glycolysis in osteoblasts, but more importantly provides evidence that increased glycolysis contributes to bone anabolism in response to PTH.

The mechanism for PTH to induce Igf signaling remains to be fully elucidated. Compared to the undifferentiated counterpart, differentiated MC3T3-E1 cells exhibit an accelerated response to PTH in both Igf1r phosphorylation and glucose consumption. On the other hand, both undifferentiated and differentiated MC3T3-E1 cells express similar levels of Igf1 or Igf2 mRNA either under basal conditions or in response to PTH. Thus, additional mechanisms are at work to mediate the faster response to PTH in the differentiated cells. For instance, PTH may promote the release of Igf1 protein preferentially in the differentiated MC3T3-E1 cells. The preferential utilization of such a mechanism in the differentiated cells may be attributable to the more robust induction of cAMP levels in those cells.[28] How cAMP induces either the production or release of Igf1 is not unclear at present, but PKA does not appear to be a critical effector because the inhibitor H89 does not impair the induction of either Igf1 mRNA or glucose consumption by PTH. Regardless of the mechanism, the stimulation of Igf1 production and release is likely to be physiologically relevant because PTH has been shown to increase bone matrix–associated Igf1 in vivo.[32] Moreover, recent studies have shown that Igf1 released from the bone matrix upon bone resorption stimulates osteoblast differentiation during bone remodeling.[33] Thus, in the intact body, PTH may exert its bone anabolic effect through both de novo synthesis of Igf1 by osteoblast-lineage cells and resorption-mediated release of Igf1 from the bone matrix.

In addition to aerobic glycolysis, PTH also stimulates oxidative phosphorylation in MC3T3-E1 cells. Paradoxically, PTH reduces the glucose flux entering the TCA cycle, indicating that an alternative nutrient fuels the increased ATP production by mitochondria. We have recently shown that Wnt signaling, which similarly stimulates aerobic glycolysis in osteoblast-lineage cells, enhances glutamine catabolism via the TCA cycle.[34] Therefore, it will be of great interest to determine whether PTH similarly promotes energy production from glutamine. In addition, the relationship between the increase in aerobic glycolysis and that in oxidative phosphorylation is unknown at present. We show that Igf1 induces aerobic glycolysis ahead of oxidative phosphorylation in differentiated MC3T3-E1 cells, but future

experiments are necessary to discern a potential causal relationship between the two processes.

It is worth noting that a brief period of PTH exposure is sufficient to induce the metabolic changes. For instance, MC3T3-E1 cells pulsed with PTH for 1 hour exhibit clear metabolic changes at a later time point. Similarly, one bolus of PTH, known to have a half-life of about 1 hour when injected subcutaneously, is sufficient to increase the protein levels of key glycolytic enzymes. Thus, the acute nature of the metabolic regulation is in line with the efficacy of intermittent dosing of PTH in promoting bone formation. Overall, the present study, together with our previous work, has uncovered the increase in aerobic glycolysis as a common feature shared by bone anabolic signals such as Wnt, PTH, and Igf1. A comprehensive understanding of such metabolic reprogramming may reveal novel targets for developing bone anabolic drugs.

Supplementary Material

Refer to Web version on PubMed Central for supplementary material.

Acknowledgments

This work is supported by NIH grants AR060456, AR055923 (FL), and P30 AR057235 (Washington University Musculoskeletal Research Center).

References

1. Hodsman AB, Bauer DC, Dempster DW, et al. Parathyroid hormone and teriparatide for the treatment of osteoporosis: a review of the evidence and suggested guidelines for its use. Endocr Rev. 2005; 26(5):688–703. [PubMed: 15769903]
2. Jilka RL. Molecular and cellular mechanisms of the anabolic effect of intermittent PTH. Bone. 2007; 40(6):1434–46. [PubMed: 17517365]
3. Bellido T, Ali AA, Plotkin LI, et al. Proteasomal degradation of Runx2 shortens parathyroid hormone-induced anti-apoptotic signaling in osteoblasts. A putative explanation for why intermittent administration is needed for bone anabolism. J Biol Chem. 2003; 278(50):50259–72. [PubMed: 14523023]
4. Kim SW, Pajevic PD, Selig M, et al. Intermittent parathyroid hormone administration converts quiescent lining cells to active osteoblasts. J Bone Miner Res. 2012; 27(10):2075–84. [PubMed: 22623172]
5. Dobnig H, Turner RT. Evidence that intermittent treatment with parathyroid hormone increases bone formation in adult rats by activation of bone lining cells. Endocrinology. 1995; 136(8):3632–8. [PubMed: 7628403]
6. Potts JT. Parathyroid hormone: past and present. J Endocrinol. 2005; 187(3):311–25. [PubMed: 16423810]
7. Gesty-Palmer D, Chen M, Reiter E, et al. Distinct beta-arrestin- and G protein-dependent pathways for parathyroid hormone receptor-stimulated ERK1/2 activation. J Biol Chem. 2006; 281(16): 10856–64. [PubMed: 16492667]
8. Li X, Liu H, Qin L, et al. Determination of dual effects of parathyroid hormone on skeletal gene expression in vivo by microarray and network analysis. J Biol Chem. 2007; 282(45):33086–97. [PubMed: 17690103]
9. Wan M, Yang C, Li J, et al. Parathyroid hormone signaling through low-density lipoprotein-related protein 6. Genes Dev. 2008; 22(21):2968–79. [PubMed: 18981475]

10. Wan M, Li J, Herbst K, et al. LRP6 mediates cAMP generation by G protein-coupled receptors through regulating the membrane targeting of Galpha(s). Sci Signal. 2011; 4(164):ra15. [PubMed: 21406690]
11. Qiu T, Wu X, Zhang F, Clemens TL, Wan M, Cao X. TGF-beta type II receptor phosphorylates PTH receptor to integrate bone remodelling signalling. Nat Cell Biol. 2010; 12(3):224–34. [PubMed: 20139972]
12. McCarthy TL, Centrella M, Canalis E. Parathyroid hormone enhances the transcript and polypeptide levels of insulin-like growth factor I in osteoblast-enriched cultures from fetal rat bone. Endocrinology. 1989; 124(3):1247–53. [PubMed: 2645113]
13. Linkhart TA, Mohan S. Parathyroid hormone stimulates release of insulin-like growth factor-I (IGF-I) and IGF-II from neonatal mouse calvaria in organ culture. Endocrinology. 1989; 125(3): 1484–91. [PubMed: 2759029]
14. McCarthy TL, Centrella M, Canalis E. Cyclic AMP induces insulin-like growth factor I synthesis in osteoblast-enriched cultures. J Biol Chem. 1990; 265(26):15353–6. [PubMed: 1697590]
15. Bikle DD, Sakata T, Leary C, et al. Insulin-like growth factor I is required for the anabolic actions of parathyroid hormone on mouse bone. J Bone Miner Res. 2002; 17(9):1570–8. [PubMed: 12211426]
16. Miyakoshi N, Kasukawa Y, Linkhart TA, Baylink DJ, Mohan S. Evidence that anabolic effects of PTH on bone require IGF-I in growing mice. Endocrinology. 2001; 142(10):4349–56. [PubMed: 11564695]
17. Wang Y, Nishida S, Boudignon BM, et al. IGF-I receptor is required for the anabolic actions of parathyroid hormone on bone. J Bone Miner Res. 2007; 22(9):1329–37. [PubMed: 17539737]
18. Esen E, Long F. Aerobic glycolysis in osteoblasts. Curr Osteoporos Rep. 2014; 12(4):433–8. [PubMed: 25200872]
19. Regan JN, Lim J, Shi Y, et al. Up-regulation of glycolytic metabolism is required for HIF1alpha-driven bone formation. Proc Natl Acad Sci U S A. 2014; 111(23):8673–8. [PubMed: 24912186]
20. Esen E, Chen J, Karner CM, Okunade AL, Patterson BW, Long F. WNT-LRP5 signaling induces Warburg effect through mTORC2 activation during osteoblast differentiation. Cell Metab. 2013; 17(5):745–55. [PubMed: 23623748]
21. Borle AB, Nichols N, Nichols G Jr. Metabolic studies of bone in vitro. II. The metabolic patterns of accretion and resorption. J Biol Chem. 1960; 235:1–211. [PubMed: 14445588]
22. Neuman WF, Neuman MW, Brommage R. Aerobic glycolysis in bone: lactate production and gradients in calvaria. Am J Physiol. 1978; 234(1):C41–50. [PubMed: 623240]
23. Rodan GA, Rodan SB, Marks SC Jr. Parathyroid hormone stimulation of adenylate cyclase activity and lactic acid accumulation in calvaria of osteopetrotic (ia) rats. Endocrinology. 1978; 102(5): 1501–5. [PubMed: 217627]
24. Long F, Joeng KS, Xuan S, Efstratiadis A, McMahon AP. Independent regulation of skeletal growth by Ihh and IGF signaling. Dev Biol. 2006; 298(1):327–33. [PubMed: 16905129]
25. Chen J, Long F. beta-catenin promotes bone formation and suppresses bone resorption in postnatal growing mice. J Bone Miner Res. 2013; 28(5):1160–9. [PubMed: 23188722]
26. Chen J, Holguin N, Shi Y, Silva MJ, Long F. mTORC2 signaling promotes skeletal growth and bone formation in mice. J Bone Miner Res. Feb; 2015 30(2):369–78. [PubMed: 25196701]
27. Reitzer LJ, Wice BM, Kennell D. Evidence that glutamine, not sugar, is the major energy source for cultured HeLa cells. J Biol Chem. 1979; 254(8):2669–76. [PubMed: 429309]
28. McCauley LK, Koh AJ, Beecher CA, Cui Y, Rosol TJ, Franceschi RT. PTH/PTHrP receptor is temporally regulated during osteoblast differentiation and is associated with collagen synthesis. J Cell Biochem. 1996; 61(4):638–47. [PubMed: 8806088]
29. Tahimic CG, Wang Y, Bikle DD. Anabolic effects of IGF-1 signaling on the skeleton. Front Endocrinol. 2013; 4:6.
30. Hernandez-Sanchez C, Blakesley V, Kalebic T, Helman L, LeRoith D. The role of the tyrosine kinase domain of the insulin-like growth factor-I receptor in intracellular signaling, cellular proliferation, and tumorigenesis. J Biol Chem. 1995; 270(49):29176–81. [PubMed: 7493944]

31. Garcia-Martinez JM, Alessi DR. mTOR complex 2 (mTORC2) controls hydrophobic motif phosphorylation and activation of serum- and glucocorticoid-induced protein kinase 1 (SGK1). Biochem J. 2008; 416(3):375–85. [PubMed: 18925875]

32. Pfeilschifter J, Laukhuf F, Muller-Beckmann B, Blum WF, Pfister T, Ziegler R. Parathyroid hormone increases the concentration of insulin-like growth factor-I and transforming growth factor beta 1 in rat bone. J Clin Invest. 1995; 96(2):767–74. [PubMed: 7635970]

33. Xian L, Wu X, Pang L, et al. Matrix IGF-1 maintains bone mass by activation of mTOR in mesenchymal stem cells. Nat Med. 2012; 18(7):1095–101. [PubMed: 22729283]

34. Karner CM, Esen E, Okunade AL, Patterson BW, Long F. Increased glutamine catabolism mediates bone anabolism in response to Wnt signaling. J Clin Invest. Feb; 2015 125(2):551–62. [PubMed: 25562323]

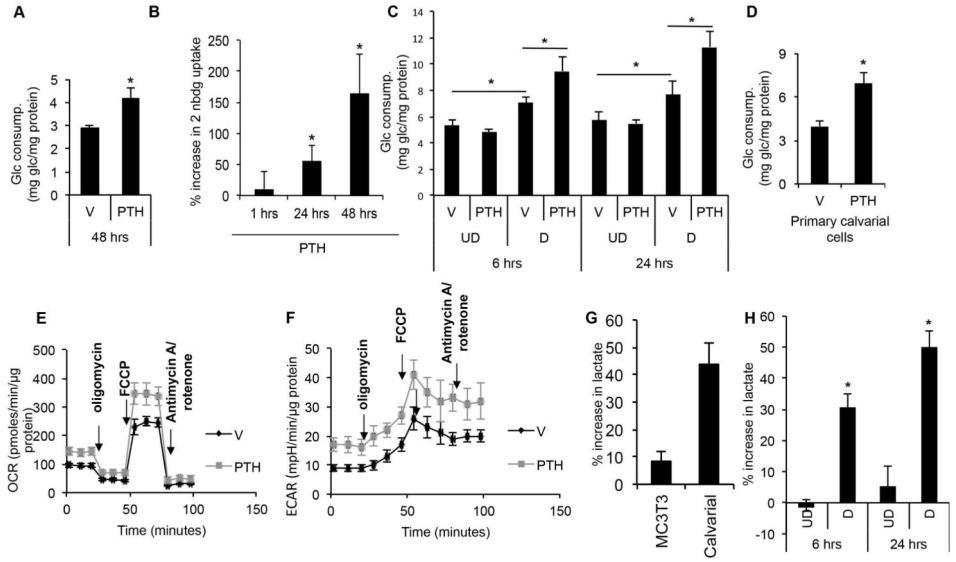

Fig. 1.

PTH stimulates aerobic glycolysis in osteoblast-lineage cells. (*A*) Glucose consumption by MC3T3-E1 cells after vehicle (V) or PTH (250 ng/mL) treatment for 48 hours. (*B*) Time-dependent increase in 2-NBDG uptake by MC3T3-E1 cells following PTH (250 ng/mL) treatment. Shown as % increase over vehicle control normalized to protein content. (*C*) Glucose consumption by undifferentiated (UD) or differentiated (D) MC3T3-E1 cells after incubation with vehicle (V) or PTH (500 ng/mL) for 6 or 24 hours. (*D*) Glucose consumption by primary calvarial cells after incubation with vehicle (V) or PTH (250 ng/mL) for 24 hours. (*E, F*) Oxygen consumption rate (OCR) (*E*) or extracellular acidification rate (ECAR) (*F*) after 24 hours of PTH (500 ng/mL) or vehicle (V) treatment. (*G*) Increase in lactate concentration in media after PTH (500 ng/mL) treatment of MC3T3-E1 or primary calvarial cells for 48 hours. Shown as % increase over vehicle control normalized to protein content. (*H*) Increase in lactate concentration in media after PTH (500 ng/mL) treatment of undifferentiated (UD) or differentiated (D) MC3T3-E1 cells for 6 or 24 hours. Shown as % increase over vehicle control normalized to protein content. *$p < 0.05$, $n = 3$. Error bars = SD. Glc = glucose; V = vehicle; UD = undifferentiated; D = differentiated; OCR = oxygen consumption rate; ECAR = extracellular acidification rate; FCCP = carbonyl cyanide p-trifluoromethoxyphenylhydrazone; 2-NBDG = fluorescent deoxyglucose derivative.

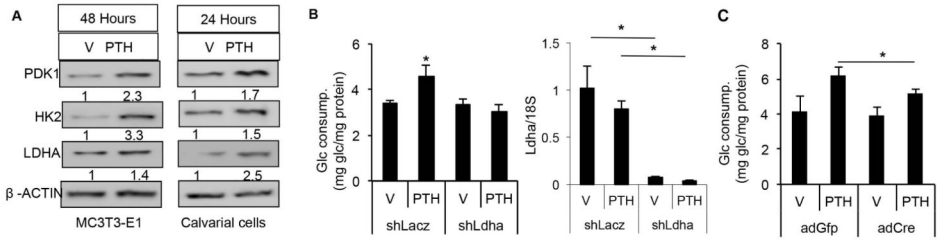

Fig. 2.

PTH increases protein levels of glycolytic enzymes. (*A*) Western blots showing the levels of indicated enzymes in MC3T3-E1 (left) or primary calvarial cells (right) treated with vehicle (V) or PTH for indicated time. Relative protein abundance normalized to β-actin. (*B*) Glucose consumption by MC3T3-E1 cells treated with vehicle (V) or PTH (500 ng/mL) for 48 hours following LDHA knockdown (shLdha) with shLacZ as control. Right panel shows relative mRNA levels of Ldha normalized to 18S rRNA as assayed by qPCR. (*C*) Glucose consumption by primary calvarial cell prepared from $Ldha^{f/f}$ mice treated with vehicle (V) or PTH (500 ng/mL) for 48 hours following infection of adenovirus expression GFP (ad-GFP) or Cre (ad-Cre). $*p < 0.05$, $n = 3$. Error bars = SD. V = vehicle; Glc = glucose.

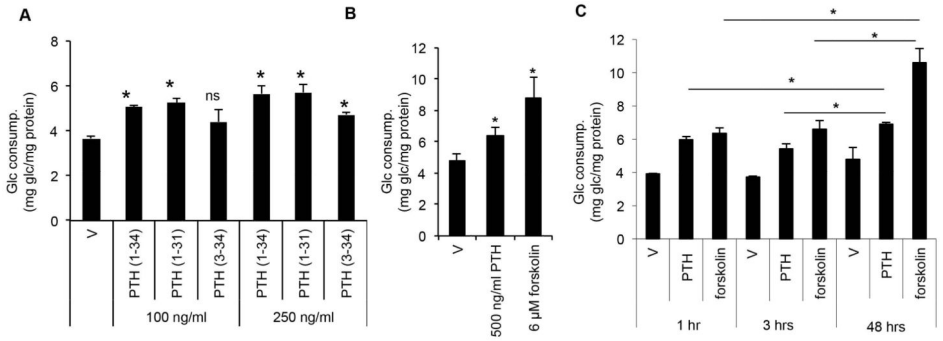

Fig. 3.

PTH stimulates glucose consumption through cAMP signaling. (*A*, *B*) Glucose consumption by MC3T3-E1 cells after treatment with vehicle (V), various PTH fragments or forskolin for 48 hours. (*C*) Glucose consumption by MC3T3-E1 cells pulsed with vehicle (V), PTH (500 ng/mL) or forskolin (6 μM) for indicated time, and harvested after a total of 48 hours in culture. $*p < 0.05$, $n = 3$. Error bars = SD. V = vehicle; Glc = glucose.

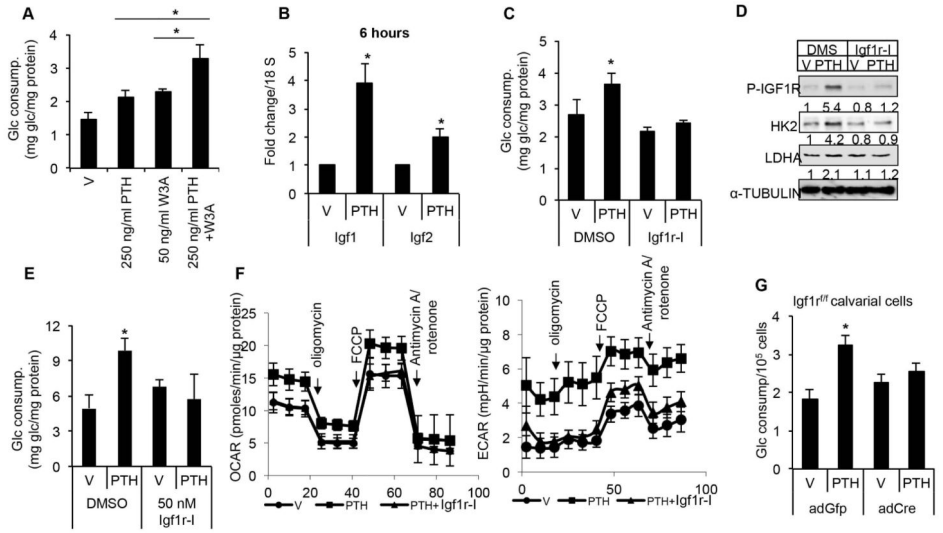

Fig. 4.

PTH stimulates glucose consumption through Igf signaling. (*A*) Glucose consumption by MC3T3-E1 cells after PTH (250 ng/mL) or Wnt3a (50 ng/mL) or combined treatment for 48 hours. (*B*) qPCR analyses of Igf1 and Igf2 mRNA in MC3T3-E1 cells treated with PTH (500 ng/mL) for 6 hours. (*C*, *D*) Effect of Igf1r inhibitor Linsitinib (100 nM) (Igf1r-I) on glucose consumption (*C*) or glycolytic enzymes (*D*) in MC3T3-E1 cells treated with vehicle (V) or PTH (500 ng/mL) for 48 hours. (*E*) Effect of Linsitinib (50 nM) on glucose consumption by differentiated MC3T3-E1 cells treated with vehicle (V) or PTH (500 ng/mL) for 48 hours. (*F*) Effect of Linsitinib (100 nM) on oxygen consumption rate (OCR) (left) or extracellular acidification rate (ECAR) (right) in differentiated MC3T3 cells treated with PTH (500 ng/mL) for 24 hours. (*G*) Glucose consumption by primary calvarial cells prepared from $Igf1r^{f/f}$ mice treated with vehicle (V) or PTH (500 ng/mL) for 48 hours following infection of adenovirus expression GFP (ad-GFP) or Cre (ad-Cre). $*p < 0.05$, $n = 3$. Error bars = SD. V = vehicle; FCCP = carbonyl cyanide p-trifluoromethoxyphenylhydrazone; OCR = oxygen consumption rate; ECAR = extracellular acidification rate.

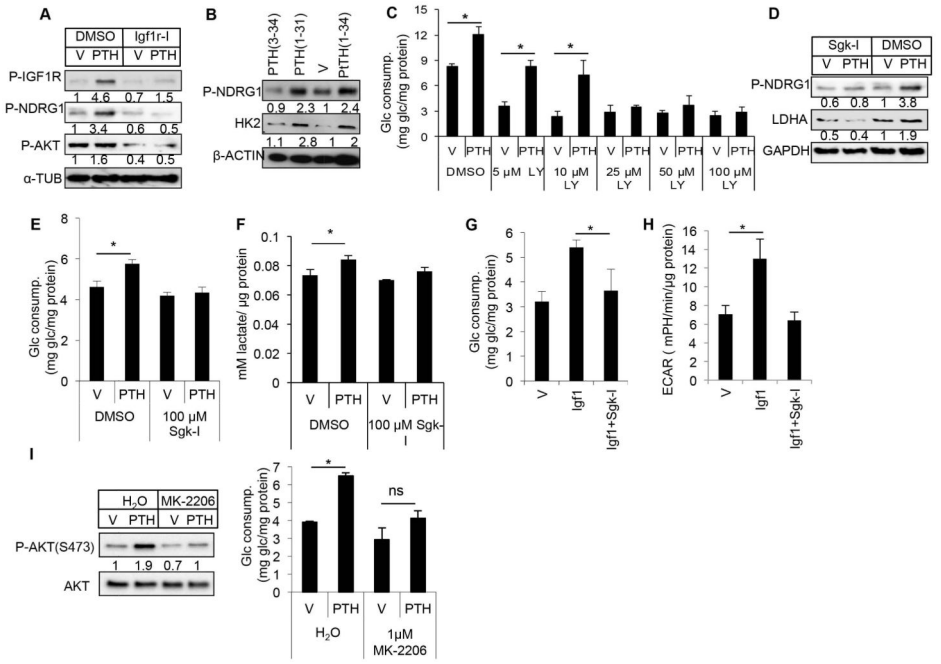

Fig. 5.

PTH stimulates glycolysis through Igf-Sgk1 signaling. (*A*) Effect of Linsitinib (Igf1r-I, 100 nM) on mTORC2 signaling in MC3T3-E1 cells in response to PTH (500 ng/mL) for 48 hours. (*B*) Western blot analyses of Sgk1 activation and HK2 accumulation in MC3T3-E1 cells treated with various PTH fragments (250 ng/mL) for 48 hours. (*C*) Effect of PI3K inhibitor LY294002 (LY) on glucose consumption by MC3T3-E1 cells treated with vehicle (V) or PTH (500 ng/mL) for 48 hours. (*D–F*) Effects of 100 μM Sgk1 inhibitor GSK650394 (Sgk-I) on MC3T3-E1 cells treated with vehicle (V) or PTH (500 ng/mL) for 48 hours. Protein abundance normalized to GAPDH in *D*. (*G*) Glucose consumption by MC3T3-E1 cells treated with vehicle (V), Igf1 (500 ng/mL) and GSK650394 (100 μM, Sgk-I) for 48 hours. (*H*) Measurements of ECAR in differentiated MC3T3-E1 cells treated for 6 hours. (*I*) Effect of AKT inhibitor MK2206 (MK) (1 μM) on P-AKT (S473) and glucose consumption by MC3T3-E1 cells treated with vehicle (V) or PTH (500 ng/mL) for 48 hours. P-AKT normalized to total AKT. $*p < 0.05$, $n = 3$. Error bars = SD. V = vehicle; Glc = glucose; LY = LY294002; ECAR = extracellular acidification rate.

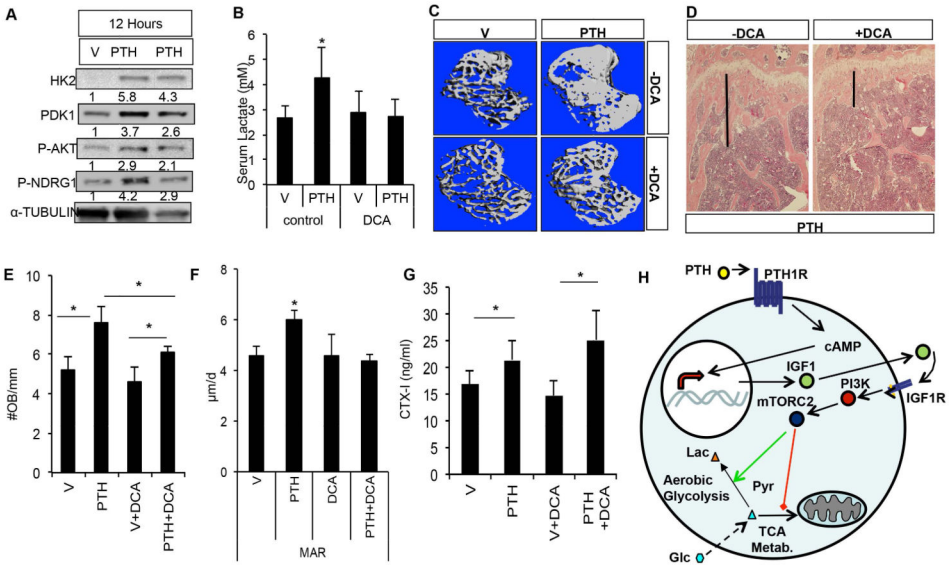

Fig. 6.

Aerobic glycolysis contributes to the anabolic effect of PTH in vivo. (*A*) Western blot analyses of bone protein extracts from mice treated with vehicle (V) or PTH (200 μg/kg) for 12 hours. Samples from two PTH-treated mice are shown. Protein abundance normalized to α-tubulin. (*B*) Serum lactate levels in mice administered vehicle (V) or PTH with or without DCA for 1 month. (*C*, *D*) Effect of PTH and DCA on trabecular bone of the proximal tibia, as analyzed by μCT (*C*) or histology (*D*). Black line denotes height of trabecular bone region. (*E*) Quantification of osteoblast numbers. (*F*) Quantification of MAR. (*G*) Serum CTX-I (ng/mL) levels. $n = 3$. (*H*) Model for PTH to reprogram glucose metabolism via Igf signaling. In addition to transcriptional upregulation of Igf1, PTH may also employ other mechanisms to activate Igf signaling (see Discussion). Green arrow = stimulation; red line = suppression. Dotted arrow symbolizes multiple steps of glycolysis. Lac = lactate; Pyr = pyruvate; Glc = glucose; V = vehicle; MAR = mineral apposition rate; DCA = dichloroacetate; OB = osteoblast; TCA = tricarboxylic acid; mTORC2 = mammalian target of rapamycin complex 2.

Table 1

$^{14}CO_2$ Production From ^{14}C-Labeled Glucose in Differentiated MC3T3-E1 Cells

	Vehicle				PTH			
^{14}C position	**$C_{3,4}$**	**C_6**	**C_1**	**C_1-C_6**	**$C_{3,4}$**	**C_6**	**C_1**	**C_1-C_6**
$^{14}CO_2$ radioactivity (dpm)	39475.6 ± 10275.9	7543.9 ± 1157.7	11281.3 ± 1599.5	6525.5 ± 1599.5	21952.8 ± 5428.4	4755.7 ± 398.6	16575.8 ± 3529.9	11820.1 ± 3529.9
Total radioactivity uptake (dpm)	214263.6 ± 46184.9	212074.4 ± 28164.9	239483.7 ± 27663.2	NA	308221.2 ± 34586.9	304272.8 ± 29502.5	339508.4 ± 25983.7	NA
$^{14}CO_2$ production rate (%)	19.3 ± 7.7	3.6 ± 0.7	4.7 ± 0.6	1.1 ± 0.6	7.3 ± 2.6	1.6 ± 0.2	4.9 ± 1.2	3.4 ± 1.2
$^{14}CO_2$ production index (%/10^6 cells)	43.9 ± 17.6	8.2 ± 1.7	10.8 ± 1.4	2.5 ± 1.4	17.2 ± 6.2	3.6 ± 0.5	11.6 ± 3.1	7.9 ± 2.9

Values are mean ± SD; $n = 4$ or 5.

Radioactivity uptake = 444,000 dpm × % glucose consumption; $^{14}CO_2$ production rate (%) = $^{14}CO_2$ radioactivity/total radioactivity uptake; $^{14}CO_2$ production index (%/10^6 cells) = $^{14}CO_2$ production rate/cell number.

Table 2

μCT Analyses of Trabecular Bone in Proximal Tibia

Group	BV/TV (%)	Tb.N (1/mm)[a]	Tb.Th (mm)[a]	Tb.Sp (mm)[a]
Vehicle	27.16 ± 3.8	5.17 ± 0.5	0.07 ± 0.0062	0.2 ± 0.034
PTH	37.52 ± 0.065 *	5.59 ± 0.36 *	0.081 ± 0.0077	0.17 ± 0.016
DCA	24.88 ± 0.078 **	5.23 ± 0.4	0.067 ± 0.01	0.19 ± 0.017
PTH+DCA	30.12 ± 0.037 ***	4.9 ± 0.38 ***	0.075 ± 0.0045	0.19 ± 0.17

Values are mean ± SD.

BV = bone volume; TV = total volume; Tb.N = trabecular number; Tb.Th = trabecular thickness; Tb.Sp = trabecular spacing; DCA = dichloroacetate.

[a] Data obtained from 35 of 16-mm slices right below growth plate, $n \geq 8$ for each group.

* Statistically significant effects for PTH were determined by ANOVA.

** Statistically significant effects for DCA were determined by ANOVA.

*** Statistically significant effects for DCA-PTH interaction were determined by ANOVA.

Table 3

μCT Analyses of Cortical Bone in Tibia

Group	BV (mm^3)	TV (mm^3)	BV/TV (%)	Cortical Th (mm)[a]
Vehicle	0.74 ± 9.133	1.1 ± 0.19	0.65 ± 0.015	0.25 ± 0.009
PTH	0.80 ± 0.078	1.13 ± 0.0087	0.70 ± 0.0052	0.27 ± 0.006
DCA	0.71 ± 0.13	1.057 ± 0.185	0.67 ± 0.019	0.26 ± 0.02
PTH+DCA	0.78 ± 0.14	1.17 ± 0.19	0.65 ± 0.029	0.26 ± 0.017

Values are mean ± SD. No statistical significance detected by ANOVA for PTH, DCA, or DCA-PTH interaction effect.

BV = bone volume; TV = total volume; Cortical Th = cortical thickness; DCA = dichloroacetate.

[a]Cortical Th data obtained from 50 of 16-mm slices at midshaft, $n = 5$ for each group.